Binding Energy of Cylindrical Quantum Dots: Effects of External Electric Field and Impurity Position

Muharrem KIRAK[1*], Sait YILMAZ[2]

[1]Yozgat Bozok University, Faculty of Education, Department of Mathematics and Science Education, 66100, Yozgat, Turkiye
[2]Yozgat Bozok University, Faculty of Arts and Sciences, Department of Physics, 66100, Yozgat, Turkiye

Abstract

We have investigated the binding energy properties of a cylindrical quantum dot (CQD) system layered as GaAs/AlGaAs under external electric fields. In our numerical calculations, we considered both on- and off-center impurity cases using the effective mass approximation. The eigenvalues and corresponding eigenfunctions of the system are obtained using a three-dimensional finite difference approach. It is found that the ground-state binding energy is significantly affected by the CQD dimensions (radius and height), impurity position, and the strength and direction of the external electric field. Additionally, the electron probability distributions are examined to provide deeper insight into the physical reasons underlying the behavior of the binding energy. These findings enhance our understanding of the tunable properties of CQDs, which may be useful in the design of optoelectronic and quantum devices.

Keywords: Electric Field, Cylindrical Quantum Dot, Impurity Position, Binding Energy

1. INTRODUCTION

Quantum dots (QDs) have become a significant focus of research in nanotechnology due to their unique quantum confinement effects. These nanostructures confine charge carriers in all three spatial dimensions, leading to discrete energy levels similar to those observed in atoms. This behavior has led to the label "artificial atoms" for quantum dots, making them useful in various optoelectronic and quantum computing applications. Among the various types of quantum dots, cylindrical quantum dots (CQDs) have garnered attention due to their symmetry and the possibility of controlling their properties through external factors such as electric fields.

Numerous studies have explored the effects of electric fields on impurity binding energy in quantum dots. For instance, K. El-Bakkari et al. [1] have numerically investigated the binding energy and diamagnetic susceptibility of impurities in multilayer cylindrical quantum dots under hydrostatic pressure, showing a strong dependence on the quantum dot radius and impurity position. Hasanirokh and Naifar [2] have explored the influence of magnetic field, dielectric environment, and Rashba parameter on second- and third-harmonic generation in AlGaAs/GaAs core–shell quantum dots, highlighting significant tunability of optical properties through impurity position control. M. El Khou et al. [3] have analyzed the effects of an external electrostatic field on the electronic and optical properties of ZnS/ZnO multi-layer cylindrical quantum dots, demonstrating how varying the field strength impacts confinement energies and absorption coefficients. Sargsian et al. [4] have examined the energy levels and nonlinear optical properties of vertically coupled InAs/GaAs quantum dots under intense laser fields, emphasizing the role of laser parameters in modulating absorption and refractive index changes. R. Charrour [5] has systematically studied the ground state binding energy of a hydrogenic impurity in cylindrical quantum dots under a strong magnetic field, revealing the critical dependence on impurity position and dot size. Feddi et al. [6] have investigated the donor impurity binding energy in hollow cylindrical-shell quantum dots, showing that the energy increases as the shell width decreases, with notable optical implications for photoionization cross-sections. Charrour et al. [7] have studied the polaron effect on the binding energy of shallow hydrogenic impurities in cylindrical quantum dots, finding that LO phonons contribute more significantly to binding energy corrections than surface optical phonon modes.

Numerous previous studies have extensively explored the effects of electric fields, magnetic fields, and impurity positions on the binding energy and optical properties of quantum dots (QDs). However, there is a notable lack of research in the literature addressing the binding energy of both on-center and off-center impurities in coupled quantum dots (CQDs) under electric fields applied in various directions.

---

[1]https://orcid.org/0000-0003-3208-2242   [2]https://orcid.org/ 0000-0003-2752-1853

In this context, the study by Belamkadem et al. [8], which investigated the influence of an external electric field applied in different directions on wedge-shaped CQDs, serves as a foundational reference and the primary motivation for our research. By building upon this framework, our study provides a novel perspective on the subject.

This paper aims to contribute to this growing body of research by studying the binding energy of an impurity in a cylindrical quantum dot subjected to an external electric field. The study will utilize numerical methods to solve the Schrödinger equation under these conditions, considering various factors such as the dot's size, the impurity's position, and the strength of the electric field. In Section 2, theoretical framework is described. Numerical results are presented in Section 3. In last section, a conclusion is given.

2. MATERIAL AND METHODS

We consider an electron and off-center impurity confined in cylindrical quantum dot (CQD) under the electric field within the effective mass approximation (EMA). The EMA simplifies the modeling of semiconductor quantum systems by replacing the complex band structure with an effective mass that represents the carrier's motion within the material. This approximation is particularly suitable for systems with smooth potential variations and when the carrier's energy is near the conduction band minimum. In our study, this approach allows the electron's dynamics in the CQD to be modeled efficiently, while capturing the essential features of the quantum confinement and impurity interactions. Under the EMA, the Hamiltonian of the structure is given by

$$H = -\frac{\hbar^2}{2m^*}\left(\frac{1}{\rho}\frac{\partial}{\partial\rho}\left(\rho\frac{\partial}{\partial\rho}\right) + \frac{1}{\rho^2}\frac{\partial^2}{\partial\theta^2} + \frac{\partial^2}{\partial z^2}\right) + |e|F\left(\rho\cos\theta\cos\phi_F + z\sin\phi_F\right) + V_c - \frac{Ze^2}{\varepsilon r}. \tag{1}$$

Here, F is the electric field, $\hbar$ is reduced Planck constant, e is electron charge, ε and m^* are dielectric constant and effective mass, respectively. Z=1 case indicates the presence of impurity and $r = \sqrt{\rho^2 + d_i^2 - 2\rho d_i \cos(\theta - \theta_i) + (z - z_i)^2}$. The coordinates electron and donor impurity are (ρ, θ, z) and (d_i, θ_i, z_i), respectively. The confining potential V_c is taken as infinite outside the CQD and zero otherwise.

The Hamiltonian H in cylindrical coordinates is formulated by discretizing as:

Radial direction: For a grid point at $\rho = i\Delta\rho$ $\qquad\qquad (1 \leq i \leq N_\rho)$

$$\frac{\partial^2\psi}{\partial\rho^2} \approx \frac{\psi_{i+1,j,k} - 2\psi_{i,j,k} + \psi_{i-1,j,k}}{\Delta\rho^2} \tag{2}$$

Angular direction: For a grid point at $\theta = j\Delta\theta$ $\qquad\qquad (1 \leq j \leq N_\theta)$

$$\frac{\partial^2\psi}{\partial\theta^2} \approx \frac{\psi_{i,j+1,k} - 2\psi_{i,j,k} + \psi_{i,j-1,k}}{(i\rho\Delta\theta)^2} \tag{3}$$

Vertical direction: For a grid point at $z = k\Delta z$ $\qquad\qquad (1 \leq k \leq N_z)$

$$\frac{\partial^2\psi}{\partial z^2} \approx \frac{\psi_{i,j,k+1} - 2\psi_{i,j,k} + \psi_{i,j,k-1}}{(\Delta z)^2} \tag{4}$$

It is discretized on three-dimensional mesh containing $(N_\rho \times N_\theta \times N_z)$ nodes according to the finite difference approach. We split the intervals $[0, R]$, $[0, 2\pi]$ and $[0, H]$ into $(N_\rho + 1)$, $(N_\theta + 1)$, and $(N_z + 1)$ parts respectively. So, we can define step range between grid points radial, angular and vertical directions as $\Delta\rho = R/(N_\rho + 1)$, $\Delta\theta = 2\pi/(N_\theta + 1)$ and $\Delta z = H/(N_z + 1)$. Here, R and H are radius and height of the CQD structure. Schrödinger equation of the system can be discretized as:

$$(t_{i,j,k} - E)\psi_{i,j,k} + l_{i,j,k}\psi_{i+1,j,k} + lq_{i,j,k}\psi_{i-1,j,k} + g_{i,j,k}\psi_{i,j-1,k} + s_{i,j,k}\psi_{i,j+1,k} + z_{i,j,k}\psi_{i,j,k-1} + x_{i,j,k}\psi_{i,j,k+1} = 0, \tag{5}$$

with

$$t_{i,j,k} = -\frac{\hbar^2}{2m^*}\left[\frac{2}{\Delta\rho^2} + \frac{2}{i\Delta\rho^2\Delta\theta^2} + \frac{2}{\Delta z^2} - \frac{2m^*}{\hbar^2}\left(|e|F\left(\rho\cos\theta\cos\phi_F + z\sin\phi_F\right) + V_c - \frac{Ze^2}{\varepsilon r}\right)\right], \tag{6}$$

$$l_{i,j,k} = -\frac{\hbar^2}{2m^*}\left(\frac{1}{2i\Delta\rho^2} + \frac{1}{\Delta\rho^2}\right), \tag{7}$$

$$q_{i,j,k} = -\frac{\hbar^2}{2m^*}\left(-\frac{1}{2i\Delta\rho^2} + \frac{1}{\Delta\rho^2}\right), \tag{8}$$

$$x_{i,j,k} = z_{i,j,k} = -\frac{\hbar^2}{2m^*}\left(\frac{1}{\Delta z^2}\right), \tag{9}$$

$$g_{i,j,k} = s_{i,j,k} = -\frac{\hbar^2}{2m^*}\left(\frac{2}{i^2\Delta\rho^2\Delta\theta^2}\right). \tag{10}$$

After constructing the Hamiltonian matrix ($N_\rho \times N_\theta \times N_z = 20 \times 20 \times 20$), the eigenvalue problem is solved to obtain the ground state energy E_0 (without impurity) and E_{imp} (with impurity) by numerically. The binding energy is calculated as the difference between the energies of the without and with impurity cases:

$$E_B = E_0 - E_{imp}. \tag{11}$$

The grid size is chosen as a compromise between computational efficiency and solution accuracy. To validate this choice, we compared the numerically obtained ground state energy for various grid sizes with the analytically calculated energy. The results indicated that increasing the grid resolution beyond $N_\rho \times N_\theta \times N_z = 20 \times 20 \times 20$ led to negligible improvements in accuracy, with a difference of less than 1.0% in the ground state energy. Thus, the selected grid resolution of considered grid size represents an optimal balance, providing sufficient accuracy while avoiding excessive computational cost.

3. RESULTS AND DISCUSSION

Throughout the numerical calculations, we used atomic units so that $\hbar = e = m_0 = 1$ (m_0 is the mass of a free electron). The material parameters are taken as $m^* = 0.067m_0$ and $\varepsilon = 13.18$ for GaAs.

Figure 1 illustrates the binding energy E_B as a function of the radius R of a cylindrical quantum dot with a centrally located impurity. As R increases, the binding energy decreases rapidly, eventually reaching a minimal value for larger radii. This behavior can be attributed to the spatial confinement effect in quantum dots, where smaller radii result in stronger quantum confinement and thus increase the binding energy due to the more confined electron-impurity interaction. As the radius grows, the electron and impurity experience less confinement, leading to a reduction in the Coulomb interaction and a consequent decrease in binding energy.
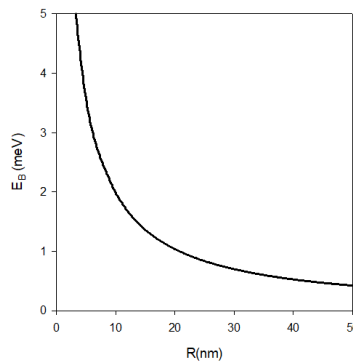

Figure 1. Binding energy E_B as a function of the radius R of a cylindrical quantum dot with on-center impurity for $H = 50nm$, $d_i = z_i = F = 0$.

Figure 2 shows the dependence of the binding energy E_B on the height H of the cylindrical quantum dot with on-center impurity. As H increases, the binding energy gradually decreases, though at a less pronounced rate compared to the radius dependence in Figure 1. This decline in binding energy with increasing height can also be explained by the reduced quantum confinement in the vertical (height)

direction. With a higher quantum dot, the electron and impurity are able to separate further along the height, diminishing the effective Coulomb interaction and reducing the binding energy, albeit with a slower reduction than observed with increasing radius.
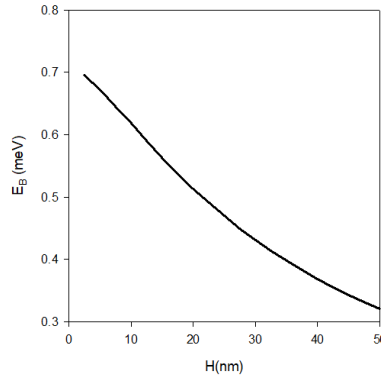

Figure 2. Binding energy E_B as a function of the height H of a cylindrical quantum dot with on-center impurity for $R = 30nm$, $d_i = z_i = F = 0$.

Figure 3(a) presents the binding energy E_B variation for a cylindrical quantum dot with an off-center impurity, focusing on the impurity's radial position, expressed as d_i/R, where d_i is the radial distance of the impurity from the center. As the impurity moves outward from the center (increasing d_i/R), the E_B decreases significantly. This reduction is primarily attributed to the weakening of the Coulomb attraction between the electron and impurity when the impurity is off-centered. Such displacement increases the average separation between the charge carriers within the dot, thereby reducing the binding energy. Figure 3(b) shows the E_B dependence on the impurity's position in the z-direction, represented as z_i/H, for a cylindrical quantum dot with an off-center impurity. In this figure, E_B reaches its maximum when the impurity is positioned near the center of the dot (around $z_i/H = 0.5$) and decreases symmetrically as the impurity moves toward the top or bottom edges. The observed trend arises from the spatial symmetry and Coulomb interaction within the dot. A central impurity position provides the strongest interaction between the electron and impurity, whereas positions closer to the edges weaken this interaction, resulting in lower binding energies.
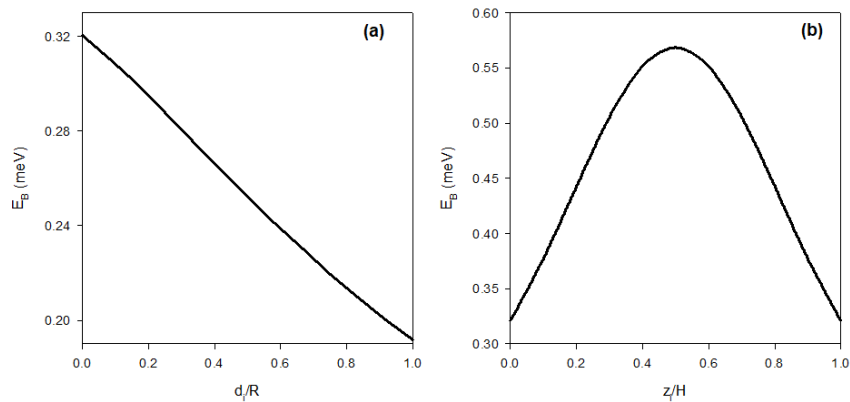

Figure 3. Binding energy E_B as a function of the impurity position (a) for d_i (b) for z_i at $R = 30nm$, $H = 50nm$ and $F = 0$.

Figures 4 depict the binding energy E_B as a function of an electric field F applied along the $\rho \cos\theta \cos\phi_F + z \sin\phi_F$ direction, with the field angles for a) $\phi_F = 0$ b) $\phi_F = \pi/2$ and c) $\phi_F = \pi$. In Figure 4(a), E_B decreases as the electric field strength increases. This behavior can be explained by the Stark effect, where the applied electric field causes a spatial separation between electron and impurity along the field direction, weakening their Coulomb attraction and thereby reducing the binding energy. The reduction is particularly evident here due to the alignment of the field with the impurity position. In Figure 4(b), as the field strength F increases, the binding energy increases linearly. This effect results from the directional alignment of the electric field with the quantum dot's vertical axis, enhancing the confinement along z-axis and increasing the electron-impurity interaction. Consequently, the binding energy rises in response to this vertical field orientation, unlike in the radial orientation. In Figure 4(c), the E_B initially increases with the electric field strength but reaches a peak and then begins to decrease. This non-monotonic behavior can be attributed to the interplay between the confinement

effect and the electric field-induced separation. Initially, the field enhances the electron-impurity attraction by aligning along the dot's vertical axis, but as the field strength grows, the Stark effect eventually dominates, causing spatial separation and thus reducing the binding energy. In the radial direction, the observed reduction in binding energy with increasing field strength can be attributed to the Stark effect, where the electric field spatially separates the electron and impurity, weakening their Coulomb interaction (Figure 4a). In the vertical direction, the field initially enhances confinement along the dot's axis, leading to an increase in binding energy; however, at higher field strengths, the Stark effect dominates, resulting in spatial separation and a subsequent decrease in binding energy (Figure 4b). In the intermediate field range, the interplay between the enhanced axial confinement and the spatial separation induced by the Stark effect produces a non-monotonic trend in binding energy (Figure 4c). Our results align with findings from Arraoui et al. [8], where binding energy reduction was reported under external fields, although their study focused on double quantum dot. Similarly, non-monotonic behavior of binding energy under varying titled angle is observed in the study of Zeng et al. [9] on ZnS/ZnO quantum dots. In this work, it is shown that the field orientation plays an important role. However, our work extends these insights by analyzing cylindrical quantum dots with variable impurity positions, offering a more comprehensive understanding of electric field-induced effects.

Figure 5 illustrates the probability density distributions for a CQD at $(d_i = z_i = 0)$ under varying electric field orientations. Figure 5a represents the unperturbed state with no applied electric field ($F = 0$), where the probability density exhibits spherical symmetry along the z-axis, consistent with the unaltered impurity potential. Figures 5 (b), (c) and (d) are plotted for $\phi_F = 0$, $\phi_F = \pi/2$ and $\phi_F = \pi$, respectively. For $\phi_F = 0$ (b), the field causes a slight elongation of the probability density, shifting the electron density towards the field's axis. At $\phi_F = \pi/2$ (c), the field induces a more pronounced asymmetry, showing a larger displacement of the density along the field orientation. In the opposite direction ($\phi_F = \pi$) (d), the density shifts in the reverse direction, demonstrating a complementary distortion. These field-induced shifts indicate the sensitivity of the quantum dot's impurity state to external electric fields, allowing manipulation of the electron's spatial distribution within the dot.
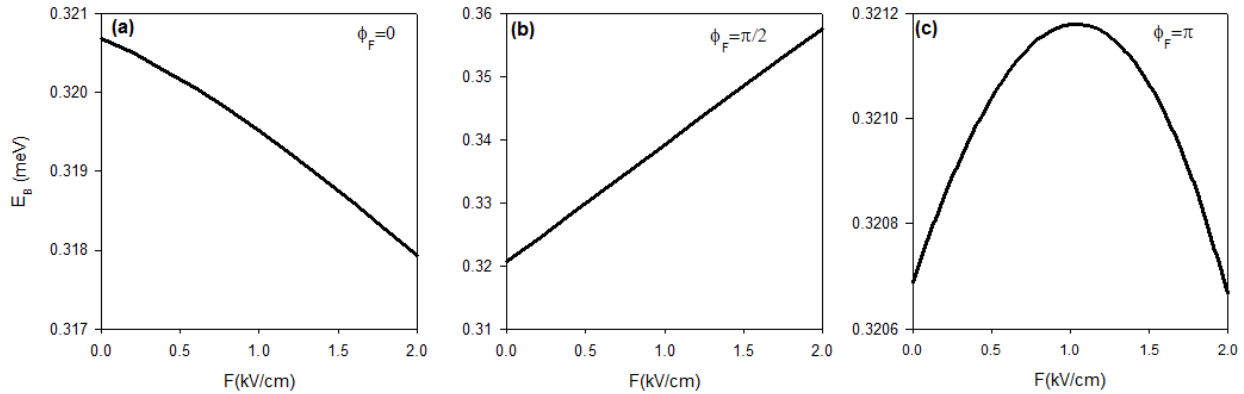

Figure 4. Binding energy E_B as a function of the electric field strength F for different directions (a) $\phi_F = 0$, (b) $\phi_F = \pi/2$ and (c) $\phi_F = \pi$ at $R = 30nm$, $H = 50nm$ and $d_i = z_i = 0$.

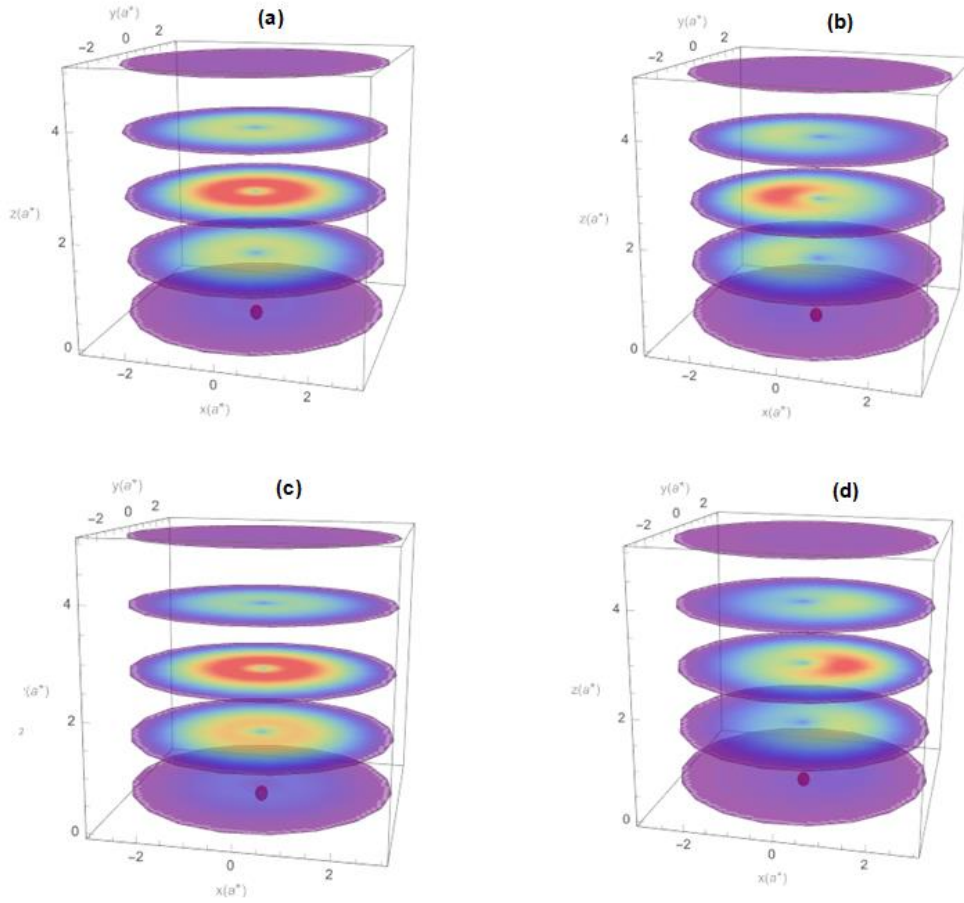Figure 5. The probability density distributions with different electric field orientations (a) $F = 0$, no electric field (b) $\phi_F = 0$, (c) $\phi_F = \pi/2$ and (d) $\phi_F = \pi$ at $R = 30nm$, $H = 50nm$ and $d_i = z_i = 0$.

4. CONCLUSIONS

This study investigates the binding energy of an impurity in a cylindrical quantum dot under the influence of an external electric field. The findings show that binding energy depends strongly on the quantum dot's dimensions, the impurity's position, and the applied electric field strength and orientation. Decreasing the dot radius or height enhances quantum confinement, thereby increasing the binding energy. Similarly, a centrally located impurity yields higher binding energy due to closer electron-impurity interaction, while an off-centered impurity diminishes this interaction and lowers the binding energy. The results also reveal the intricate impact of an external electric field on the binding energy, which varies based on field orientation. This study contributes to the understanding of impurity binding in cylindrical quantum dots, providing insights relevant to the design of optoelectronic devices where quantum confinement effects play a crucial role. Our findings highlight the tunable nature of binding energies in cylindrical quantum dots under external electric fields, providing valuable insights for the design of advanced nanostructured materials. This tunability can be exploited in the development of optoelectronic devices, such as quantum dot lasers, photodetectors, and field-effect transistors. Moreover, future research could extend these insights by exploring other material systems, different impurity types, and the influence of environmental conditions like temperature. Future work could extend these findings by examining the effects of different impurity types and considering temperature dependence, adding further depth to the study of quantum confinement and external field impacts on nanostructures.

AUTHOR'S CONTRIBUTIONS

The authors contributed equally.

CONFLICTS OF INTEREST

Authors have declared no conflict of interest

RESEARCH AND PUBLICATION ETHICS

The authors declare that this study complies with Research and Publication Ethics.

REFERENCES

[1] K. El-Bakkari, M. Jaouane, A. Fakkahi, R. Arraoui, H. Azmi and A. Sali, "Hydrogenic Donor-Related Binding Energy and Diamagnetic Susceptibility in Multilayer Cylindrical Quantum Dots under Hydrostatic Pressure," Appl. Phys. A vol. 129, pp. 557, July 2023, doi:10.1007/s00339-023-06834-4.

[2] K. Hasanirokh and A. Naifar, "Inspecting the Impact of Decisive Factors on the Second- and Third-Harmonic Generation in Cylindrical Core/Shell/Shell Quantum Dot (CCSSQD) with Hydrogenic Impurity,". Eur. Phys. J. Plus vol. 138, pp.1031, Nov. 2023, doi: 10.1140/epjp/s13360-023-04663-1.

[3] M. El Khou, M. Rzaizi, E. A. Ibnouelghazi, and D. Abouelaoualim, "Effects of an External Electric Field on the Electronic and Optical Properties of a Cylindrical ZnS/ZnO Multi-layer Quantum Dot with a Parabolic Potential," Rev. Mex. de Fisica, vol. 69, pp. 01160, August 2024, 10.31349/revmexfis.69.011601.

[4] T.A. Sargsian, P.A. Mantashyan and D. B. Hayrapetyan, "Effect of Gaussian and Bessel Laser Beams on Linear and Nonlinear Optical Properties of Vertically Coupled Cylindrical Quantum Dots," Nano-Structures & Nano-Objects, vol. 33, pp. 100936, Feb. 2023, doi: 10.1016/j.nanoso.2022.100936.

[5] R. Charrour, M. Bouhassoune, M. Fliyou and A. Nougaoui, "Magnetic Field Effect on The Binding Energy of a Hydrogenic Impurity in Cylindrical Quantum Dot," Physica B: Cond. Matt., vol. 293, pp. 137-143, Dec. 2000, doi: 10.1016/S0921-4526(00)00495-6.

[6] E. Feddi, M. El-Yadri, F. Dujardin, R. L. Restrepo and C. A. Duque, "Photoionization Cross Section and Binding Energy of Single Dopant in Hollow Cylindrical Core/Shell Quantum Dot," J. Appl. Phys., vol. 121, pp. 064303, Feb. 2017, doi: 10.1063/1.4975648.

[7] R. Charrour, M. Bouhassoune, M. Fliyou, D. Bria and A. Nougaoui, "Binding Energy of Hydrogenic Impurities in Polar Cylindrical Quantum Dot," J. Phys.: Condens. Matter, vol. 12, pp. 4817, June 2000, doi: 10.1088/0953-8984/12/22/314.

[8] L. Belamkadem, O. Mommadi, R. Boussetta, S. Chouef, M. Chnafi, A. El Moussaouy, J.A. Vinasco, D. Laroze, C.A. Duque, C. Kenfack-Sadem, R.M. Keumo Tsiaze, F.C. Fobasso Mbognou and A. Kerkour El-Miad, "The Intensity and Direction of the Electric Field Effects on Off-Center Shallow-Donor Impurity Binding Energy in Wedge-Shaped Cylindrical Quantum Dots," Thin Sol. Films, vol: 757, pp. 139396 -139410, July 2022, doi: 10.1016/j.tsf.2022.139396.

[9] R. Arraoui, A. Sali, A. Ed-Dahmouny, K. El-Bakkari, M. Jaouane and, A. Fakkahi, "The Spatial Electric Field Effect on the Impurity Binding Energy and Self-Polarizationin a Double Quantum Dot," Eur. Phys. J. Plus, vol: 137, pp. 979 -98, Aug. 2022, doi: 10.1140/epjp/s13360-022-03193-6.

[10] Z. Zeng, C. S. Garoufalis, S. Baskoutas and A. F. Terzis, "Stark Effect of Donor Binding Energy in a Self-Assembled GaAs Quantum Dot Subjected to a Tilted Electric Field," Phys. Lett. A, vol: 376, pp. 2712-2716, Aug. 2012, doi: 10.1016/j.physleta.2012.07.032.